

A centre slotted parasitic patch antenna for bandwidth enhancement on a low cost a polymer resin material substrate

M. SAMSUZZAMAN*, S. YAHAHIA, M. TARIKUL ISLAM, M. N. RAHMAN, M. T. ISLAM
Centre of Advanced Electronic and Communication Engineering, Universiti Kebangsaan, Malaysia

In this paper, a rotated square slot with parasitic centre slot printed antenna is proposed for bandwidth enhancement on low-cost polymer resin material substrate. The antenna is constructed with an I shaped microstrip feed line for exciting the radiating element and the rotating square slot with centre slotted parasitic element is implanted in the centre position of the ground plane to enhance the bandwidth. Two diagonal slots are also introduced for widened the bandwidth. The proposed antenna shows -10dB impedance bandwidth of 92.68% from a frequency of 2.20 to 6.0 GHz with the compact size of $0.26 \lambda \times 0.26 \lambda \times 0.01 \lambda$, at lower end frequency. The average gain is about 3.65 dBi with a stable omnidirectional radiation pattern in the entire operating band. Several parametric studies have been performed to analyse the physical properties of the proposed antenna. In this design, a smaller ground plane is considered compared to the reference antenna. The antenna Q-factor is analysed to verify the optimum design. The proposed antenna fulfils the requirements of the WLAN, WiMAX, ISM bands for RFID and other wideband wireless applications.

(Received April 2, 2018; accepted October 10, 2018)

Keywords: Centre square slot, Bandwidth enhancement, Microstrip-line-fed antennas, Parasitic, Q factor, Wideband

1. Introduction

Nowadays, printed slots antennas are becoming the most popular among the antenna researchers due to their wide impedance bandwidth characteristics. There are some other characteristics like the low profile, lightweight, multi-frequency capability and cost-effectiveness. In addition, a printed microstrip antenna has the flexibility to integrate with other microwave circuits and devices. However, the printed microstrip antenna has some demerits like narrow bandwidth with low gain and low power handling capability. Therefore, various researches have been doing research on the microstrip-fed printed antenna to overcome its demerits and to enhance performances [1].

Printed slot antennas have a great appeal in the diversity of communication systems due to having two orthogonal resonant modes, which simultaneously create wide impedance bandwidth [2]. Recently, antenna researchers have given the devotion to achieve wide impedance bandwidth with different shapes of slot antenna [3, 4], ellipse [5], and triangle [6]. Every slot patch requires appropriate feeding techniques. An optimum impedance bandwidth can be achieved using coupling between slot and feeding [7-14]. Sze et al. proposed a microstrip line feed with a fork-like tuning stub, which provides wide impedance bandwidth [7]. Dissanayake et al. introduced an L-shaped slot to improve impedance bandwidth in [8]. In [15, 16], microstrip feed fractal shape antennas were proposed for bandwidth enhancement. Though this technique plays a significant role to enhance bandwidth, configuration of the wide-slot antenna more

complicated. However, the square slot antenna shows wider impedance bandwidth than other types of the antennas, but the application is limited due to its single resonating mode characteristics. Mr Sung succeeded to create another resonant mode using a rotating square [17]. As a result, a wide operating bandwidth of about 2.2 GHz (49.4%) with respect to the centre frequency of 4.453 GHz was obtained. However, it is not enough for the operating bandwidth to cover more wireless communication services especially in Wi-Fi/WiMAX applications [8]. Mr Sung proposed a centre square rotating parasitic patch was used to achieve wide impedance bandwidth [9] and achieved a fractional impedance bandwidth of 80% (2.2 GHz to 5.35 GHz). The dimension of the antenna was $37 \times 37 \times 1.6 \text{ mm}^3$. There is stillroom to explorer miniature antennas with wideband, high gain and more efficient with the different material substrate. In this paper, a compact microstrip line-fed with rotated centre square slotted ground with two parasitic patches printed antenna is proposed for bandwidth enhancement. This paper uses the structure as proposed in the reference antenna [9, 17]. In this case, the overall dimension of the proposed antenna total area is $36 \text{ mm} \times 36 \text{ mm}$. It has a size reduction of about 75%, as compared to the designed antenna in [17]. A detailed simulation is conducted to understand the antenna behaviour and optimize the antenna parameters for broadband operation. The proposed antenna has been manufactured and measured the antenna parameters to validate the simulated one. The measured results show -10 dB reflection coefficient impedance bandwidth of 3.84 GHz, which indicates the improved bandwidth of the reference antenna [9] by about 720 MHz. Moreover, an

average gain of 3.65 dBi, average radiation efficiency of 92.28 % and stable omnidirectional radiation pattern has reached in the entire operating bandwidth.

In this paper, a compact microstrip line-fed with rotated centre square slotted ground with two parasitic patch printed antenna is proposed for bandwidth enhancement. This paper uses the structure as proposed in the reference antenna [9, 17]. In this case, the overall dimension of the proposed antenna total area is 36 mm×36 mm. It has a size reduction of about 75%, as compared to the designed antenna in [17]. A detailed simulation is conducted to understand the antenna behaviour and optimize the antenna parameters for broadband operation. The proposed antenna has been manufactured and measured the antenna parameters to validate the simulated one. The measured results shows -10 dB reflection coefficient impedance bandwidth of 3.84 GHz, which indicates the improved bandwidth of the reference antenna [9] by about 720 MHz. Moreover, average gain of 3.65 dBi, average radiation efficiency of 92.28 % and stable omnidirectional radiation pattern has reached in the entire operating bandwidth.

2. Antenna design architecture

Current wireless applications have challenged antenna designers with demands for low cost, high performance, easily fabricated compact multiband antennas with simple radiating elements, and signal feeding configurations. These results can be obtained by designing a modified, edge feeding slotted rectangular patch antenna.

2.1. Fundamental concepts

a) Design Specifications: The three essential parameters for the design of a patch antenna are the resonant frequency, f ; the dielectric constant of the substrate, ϵ ; and the thickness of the substrate, h . Wideband design frequencies are chosen here because they require low-cost components, are located in the S band, C band, and experience extremely low attenuation through the atmosphere. The proposed antenna fulfils the requirements of the WLAN, WiMAX, ISM bands for RFID and other wideband wireless applications.

b) Rectangular Patch Design: A rectangular microstrip patch antenna is taken as the generator of the slotted antenna. The most popular models for the analysis of microstrip patch antennas are the transmission line model, cavity model, and full-wave model (which include primarily integral equations/moment method). As the transmission line model is the simplest of these and provides a good deal of physical insight, it is adopted as the design method for the proposed antenna. In essence, the transmission line model represents a microstrip antenna as two slots, each of width W and height h , separated by a transmission line of length L . Thus, the microstrip is essentially a nonhomogeneous line of two

dielectrics—typically, the substrate and the surrounding air. The patch dimensions are calculated by following the simplified formulation of the transmission line model [1].

The width of the antenna is determined to be

$$W = \frac{c}{2f_r} \left(\frac{\epsilon_r + 1}{2} \right)^{\frac{1}{2}} \quad (1)$$

Here, ϵ_r is the permittivity of the substrate material, f_r is the resonant frequency, c is the speed of light at free space. To find the effective permittivity of the substrate the equation can be derived as:

$$\epsilon_{re} = \frac{\epsilon_r + 1}{2} + \frac{\epsilon_r - 1}{2} \left(1 + \frac{12h}{W} \right)^{-\frac{1}{2}} \quad (2)$$

Here, h is the substrate thickness. The path length (L) can be calculated as:

$$L = \frac{c}{2f_r \sqrt{\epsilon_{re}}} - 2\Delta L \quad (3)$$

c) Feeding Techniques: Antenna performance depends largely on the feeding technique and the location of the optimum feed point. Microstrip line or coaxial probe feeding is widely used in single layer antenna design because these types of feed are easy to design and fabricate. Impedance control in microstrip feeding can be obtained by either edge feeding, inset feeding, or feeding through an additional matching network called a quarter-wave transformer; in this study, microstrip line feeding is used. A microstrip line introduces a physical notch that in turn produces junction capacitance. Together, these influence the resonance frequency; as the inset feed point moves inward from the edge, the frequency decreases monotonically, reaching zero at the centre. The input impedance of an edge-fed microstrip patch antenna depends mainly on the inset distance (length of the notch) and, to a lesser extent, on the inset width (width of the notch), while the resonant frequency is much more affected by variations in the inset width than in the inset length.

2.2. Proposed antenna geometric layout

The geometry of the proposed wide slot defected ground structure antenna is depicted in Figure 1. The proposed antenna is printed on polymer resin substrate FR4 of thickness 1.6 mm and relative permittivity 4.6 with loss tangent 0.02. The antenna consists of a simple configuration with a wide rotated square slot, two rotated parasitic square slit with one square slot, in the centre of the ground of one side of the substrate. A 50-ohm microstrip-fed line is printed on the other side of the substrate for exciting two modes with the close resonance frequency. The rotated square slot has a side length of LI

which determines the lower resonant frequency. To decrease the length of $L1$, the lower resonant frequency is shifted upward. Thus, the lower edge of the operating frequency band also goes upward. This is because the decrease in length $L1$ will shorten the effective current path. Therefore, the centre of the rotated square slot is embedded in the middle of the ground plane and up and down diagonal points are in the middle of the I shaped strip line for obtaining a stable symmetric radiation pattern. Generally, it is desirable to select a stub that is parallel to the slot edges. Therefore, the centre slotted parasitic patch is oblique to the y-axis at an angle of 45 degree which is depicted in Fig. 1. The parasitic centre slotted square patch acts as the radiator as well as the feed structure for the rotated square slot antenna. The parasitic centre square patches side length are denoted by $L2$ and $L4$, respectively. The rotated slot side length also defined by $L3$. Ground plane length is denoted by G_L , slot1 width and length is denoted by $W1$, and $L5$ respectively. On the other hand slot, 2 width and length is defined by $W2$ and $L6$, respectively. Microstrip line width and length are denoted by Wf and Lf , respectively. Compare to the designed antenna in [9, 17], the proposed antenna has achieved better impedance bandwidth, gain and smaller size. The details of the optimized design parameter are summarized as follows: $G_L=36$ mm, $L1=24.04$ mm, $L2=9.19$ mm, $L3=5.65$ mm, $L4=2.83$ mm, $L5=11.47$ mm, $L6=7.23$ mm, $Wf=3.25$ mm, $Lf=15.75$ mm, $W1=2.5$ mm, $h=1.60$.

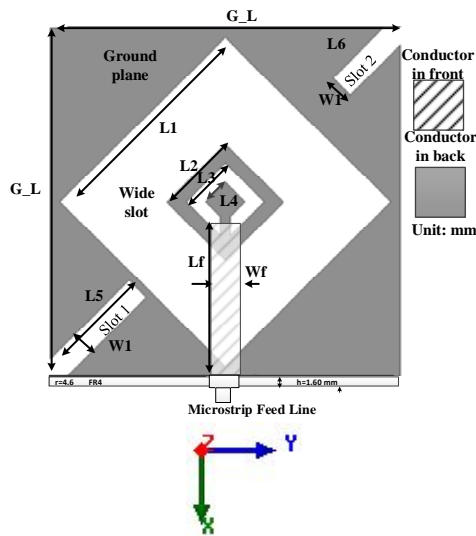


Fig. 1. Proposed antenna geometric layout

Antenna design evolution is presented in Fig. 2. It is seen from Fig. 2 that the antenna has been analyzed in seven stages. The reflection coefficient of every stage has also been investigated, presented in Fig. 3. From this figure, it can be observed that no -10 dB impedance bandwidth achieves with Antenna 1 which is just a rectangle and I shaped feed line. After etched out a rotated square slot about 1.2GHz impedance bandwidth achieves through Antenna 2. Then a centre slotted patch has

inserted to achieve wideband but middle frequency reflection coefficient still above -10dB. To minimize the reflection coefficient, a center square patch has introduced which is shown in Antenna 4. In antenna 5, two middle center patch has connected to reduce the reflection coefficient value. Finally, two diagonal rectangular slot has etched out from the ground plane to design the proposed antenna which has achieved maximum impedance bandwidth (2.20 GHz to 6.00 GHz).

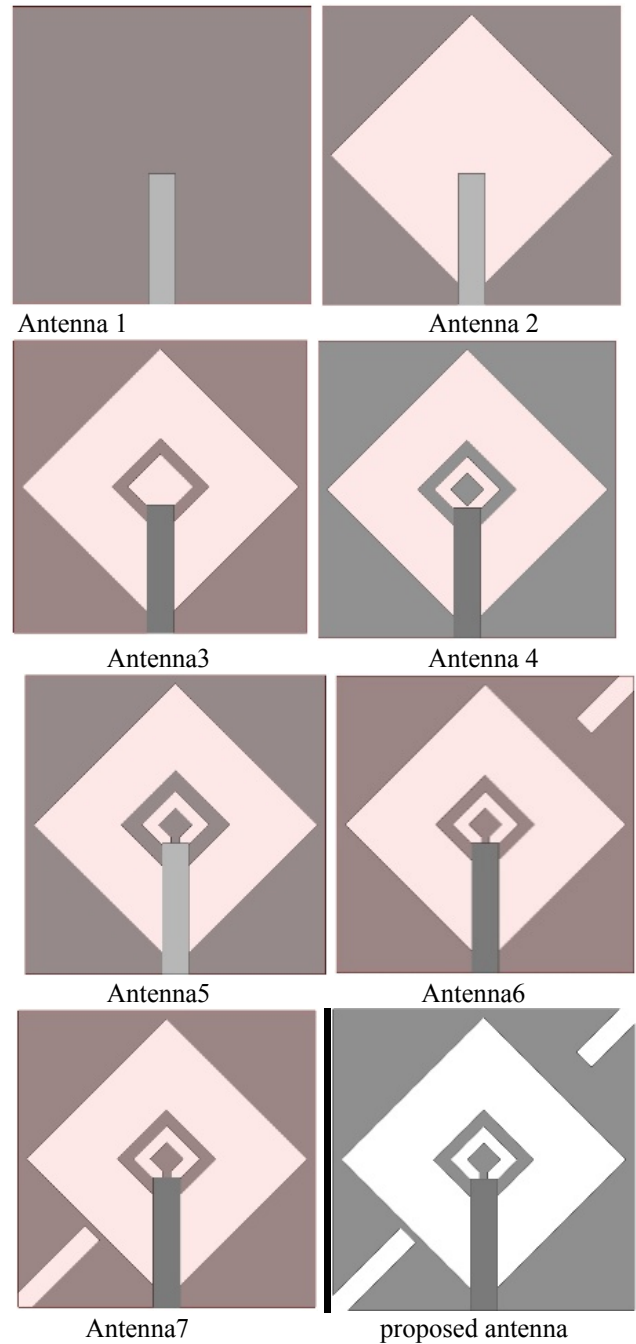


Fig. 2. Antenna evaluation procedure

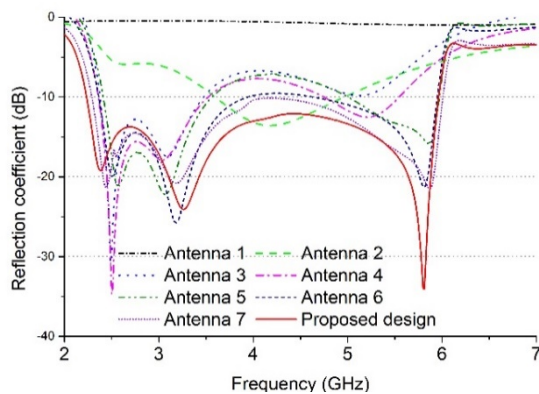


Fig. 3 Effect on the reflection coefficient for different antenna design

3. Parametric study

All critical physical parameters, such as $L1$, $L2$, $L5$, $L6$, lf , and Wf , should be adjusted carefully in order to achieve wideband impedance bandwidth. In this section, we will examine the effects of these parameters on impedance bandwidth only one parameter varying at a time. As mentioned earlier, the lower frequency is decided by the wide square slotted ground and the upper frequency is decided by the centre slotted patch.

3.1. Effects of $L1$

The rotated square slot of the antenna is made at the centre of the ground plane. The side length of square slot $L1$ along with substrate underneath is varied, and effects of which on the S_{11} characteristics is shown in Fig. 4. This is a critical parameter which decides the upper frequency. The length of slot $L1$ is varied from 18.38 to 24.04 mm. Whether the value is $L1$ is too small, the impedance bandwidth will be deteriorated. The optimized dimension of $L1$ is 24.04 mm.

3.2. Effects of $L2$

Fig. 5 shows the impedance bandwidth of the proposed antenna in the case of $L2=11.31, 9.90, 8.48, 7.77, 7.07$ mm, respectively. It is found that the impedance bandwidth of the upper frequency varies slightly with different $L2$'s, while there is an obvious variation of the impedance bandwidth of the lower and middle frequency when $L2$ increases from 7.07 to 11.31 mm. To obtain good impedance matching, o should be set to 8.48mm.

3.3. Effects of $L5$ and $L6$

Fig. 6 depicts the impedance bandwidth of the proposed antenna in the case of $L5= 8.64, 10.06, 11.47, 12.18$ mm, respectively. It is noted that the impedance bandwidth of the upper and middle frequency has less effect with different $L5$'s, while there is an obvious variation of the impedance bandwidth of the lower

frequency when $L5$ increases or decreases from optimum value 11.47mm. On the other hand, Fig. 7 shows the effect on the antenna performance of $L6$. With reference to Fig. 7, by increasing or decreasing the $L6$ value, there is no effect on lower or higher frequency, but the good variation is on middle frequency. The optimum value of $L6$ is 7.23 mm.

3.4. Effects of lf and Wf

Fig. 8 and Fig. 9 show the effects of lf and Wf , which are the length of the width of the feed line. As expected lf has a great effect on the impedance bandwidth of lower and middle frequency but Wf has an effect on middle and higher frequency. Whether the values of lf and Wf are small or large, the impedance matching will be deteriorated. To obtain good impedance matching, lf and Wf should be set as 15.75 and 3.25 mm, respectively.

3.5. Effects of substrate

The substrate material consists of an epoxy matrix reinforced by the woven glass. This composition of epoxy resin and fiber glass varies in thickness and is direction dependent. One of the attractive properties of polymer resin composites is that they can be shaped and reshaped repeatedly without losing their material properties[18]. Due to the low manufacturing cost, ease of fabrication, design flexibility and market availability of the proposed material, it has become popular for use as a substrate for patch antenna design. The composition ratio of the material is 60 % fiber glass and 40 % epoxy resin. The effect of the different substrate materials on the reflection coefficient of the proposed antenna is shown in Fig. 12. It can be clearly seen that the proposed antenna provides a wider bandwidth and acceptable return loss value compared to the other reported materials.

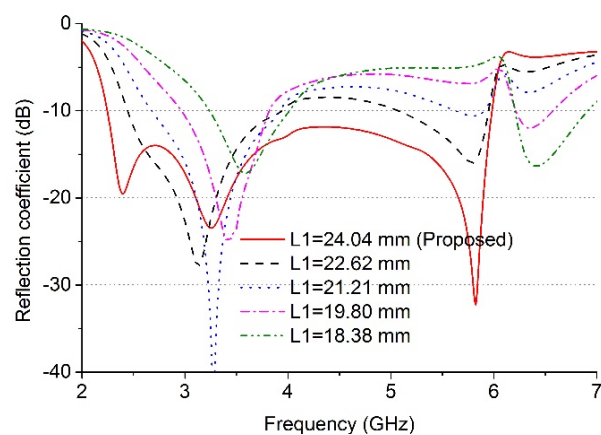


Fig. 4. Effect on the Reflection coefficient for different values of $L1$

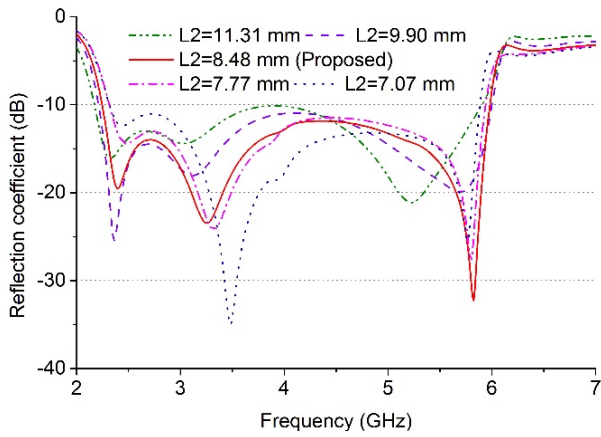


Fig. 5. Effect on the Reflection coefficient for different values of L_2

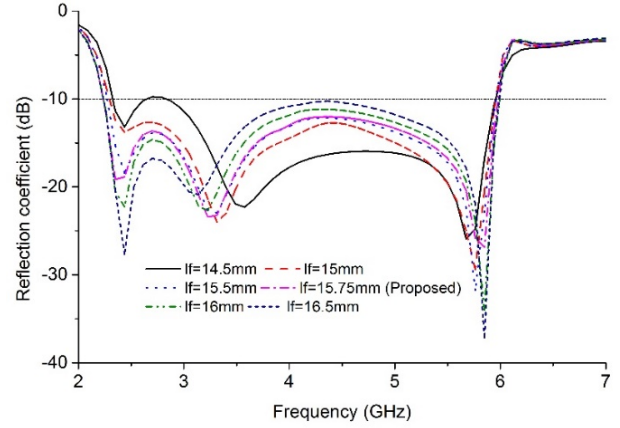


Fig. 8. Effect on the Reflection coefficient for different values of L_f

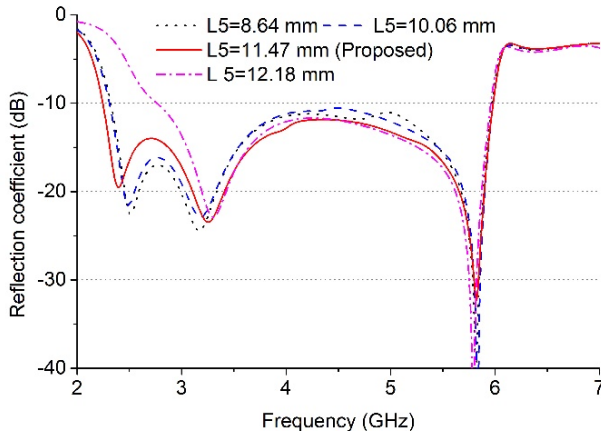


Fig. 6. Effect on the Reflection coefficient for different values of L_5

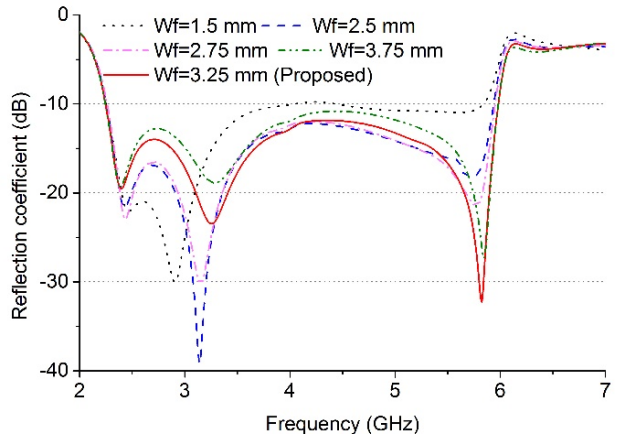


Fig. 9. Effect on the reflection coefficient for different feed width W

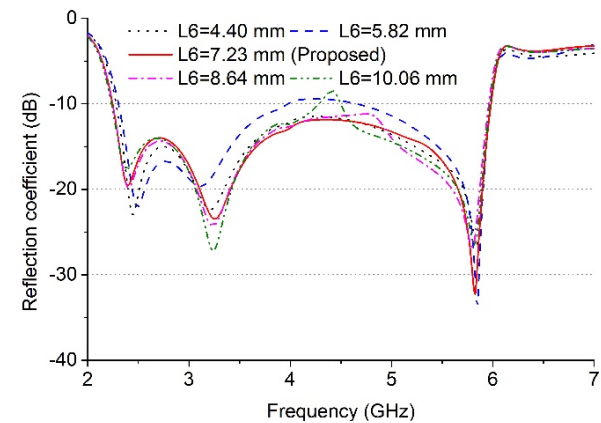


Fig. 7. Effect on the Reflection coefficient for different values of L_6

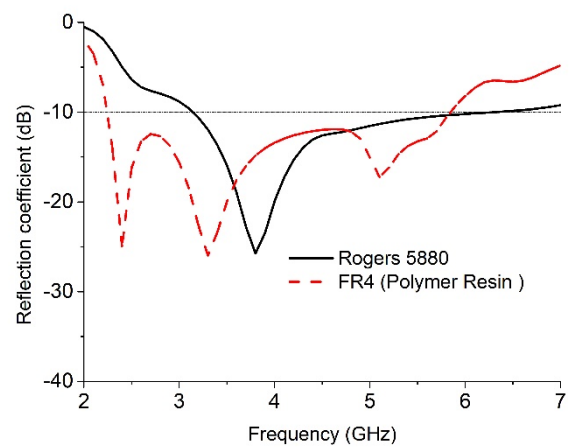


Fig. 10. Simulated reflection coefficient for different substrate materials

4. Results and discussion

The performance characteristics of the wide slot with parasitic slotted centre patch antenna have been analyzed, studied and optimized by utilizing the 3D electromagnetic structure solving functionality of ANSYS' FEM (finite element method) based HFSS simulator. The accomplishment of the parametric study gives an optimized geometric structure of the proposed antenna which is realized through in-house PCB LKPF prototyping machine to get a physical test model. Afterwards, the antenna parameters have been measured with the help of Agilent's Vector Network Analyzer (Agilent E8362C) in a standard sized anechoic measurement chamber. The photograph of the proposed antenna prototype is shown in Fig. 11. The simulated and measured return loss of the optimized proposed antenna is shown in Fig. 12. The results show the antenna provides a very wide -10dB impedance bandwidth of over 92.157% from a frequency of 2.21 to 6.05 GHz. A slight discrepancy has occurred that lead to the differences between simulated and measured return loss value due to the effect of soldering of the SMA connector and the loss from the connecting cable.

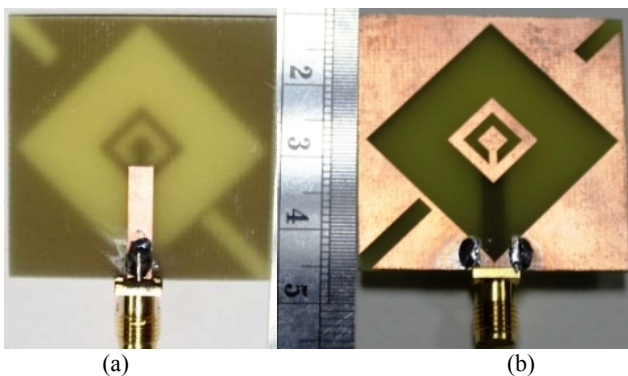


Fig. 11. Fabricated prototype a) front view b) back view

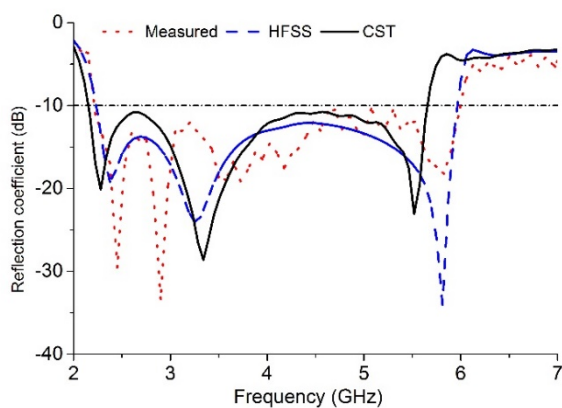


Fig. 12. Comparison between simulated and measured reflection coefficient of the proposed antenna

StarLab near-field antenna measurement system as shown in Fig. 13 is used to measure the gain, efficiency and radiation pattern of the prototype. This system allows measuring the antenna's electric fields within the near-field region with an aim to compute the corresponding far-field values of the antenna under test (AUT). The AUT, placed on the test bed, is positioned in the middle of a circular "arch" that contains 16 individual measuring probes. These probes are placed at an equal distance surrounding the circular surface. The AUT is rotated horizontally in 360° angles, and this rotation and array of probes together do a full 3D scan of AUT and collecting data for 3D radiation patterns. The far-field data is then employed to compute the gain and efficiency of the AUT.

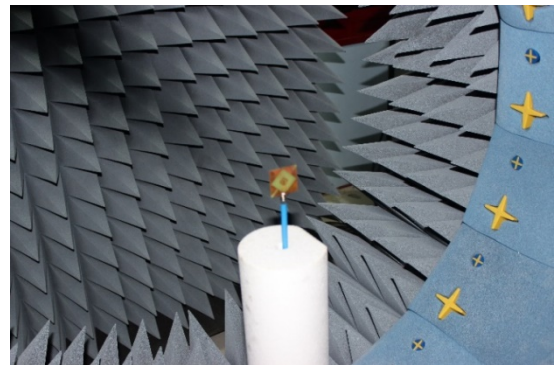


Fig. 13. Radiation characteristics measurement setup

Fig. 14 shows the surface current distribution of the radiating patch element of the proposed antenna at 2.50 GHz, 3.0 GHz, 4.2 GHz and 5.5 GHz, respectively. It has been observed that at the lower band the current intensity is much weaker. The current is more exciting in stripline and wide slotted diagonal points. Especially, the left and right arms of the wide slot are more excited. Besides, rectangle slots in the ground plane are also more excited than plane area. Therefore, from the relationship between gain, power and current of the proposed antenna can be validated from the current distribution. The simulated E-H plane normalized radiation pattern of the proposed antenna prototype is shown in Fig. 15 at different frequencies. It can be undoubtedly seen that good omnidirectional characteristics are obtained in E-plane for the proposed antenna excited at all other frequencies across the operating band. Furthermore, the effect of cross-polarization is much smaller than the co-polarization which is desired. Although at higher frequencies, more harmonics are observed mainly in cross polarization radiation field, the antenna has a good stable radiation without gain degradation.

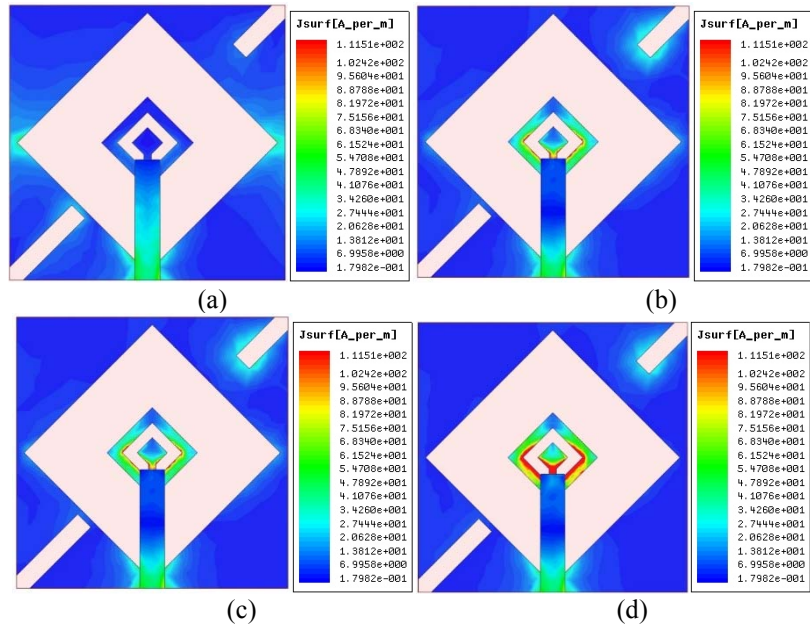


Fig. 14. Surface current distribution of the proposed antenna at a) 2.50 GHz b) 3.0 c) 4.2 GHz d) 5.5 GHz

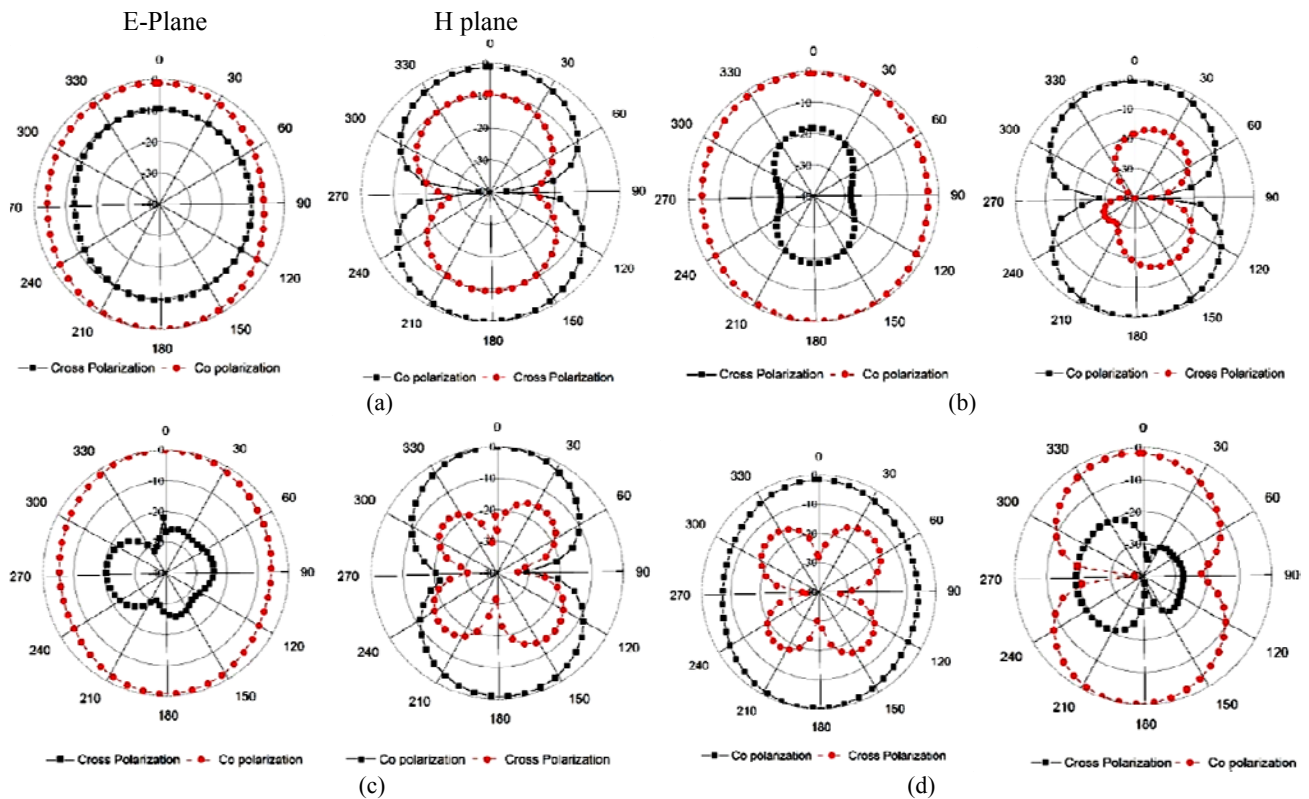


Fig. 15. Radiation pattern of the proposed antenna at a) 2.40 GHz b) 3.50 GHz c) 5.2 GHz d) 5.8 GHz

The radiation efficiency of the proposed antenna is shown in Fig.16. It can be shown at 92.58 % of average radiation efficiency is achieved in the entire operating band. The radiation efficiency at a lower resonant frequency of 3.20 GHz, 3.50 GHz, and 3.70 GHz are achieved at 92.58%, 92.04% and 91.41%, respectively. On the other hand, at the upper resonant frequencies of 5.2

GHz, 5.5 GHz and 5.8 GHz, the radiation efficiency is 89.35%, 89.56% and 89.45%, respectively.

The measured gain of the proposed antenna is depicted in Fig. 17. The average gain of the proposed antenna is obtained at 3.65 dBi. The measured smith chart of the proposed antenna is illustrated in Fig. 18. It is seen

from Fig. 18 that the input impedance of the proposed antenna matches well.

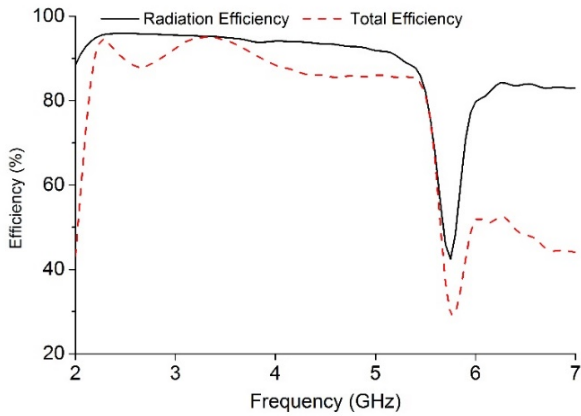


Fig. 16. Radiation efficiency of the proposed antenna

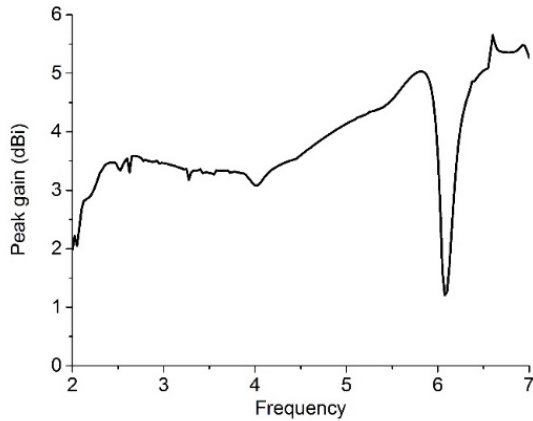


Fig. 17. Measured gain of the proposed antenna

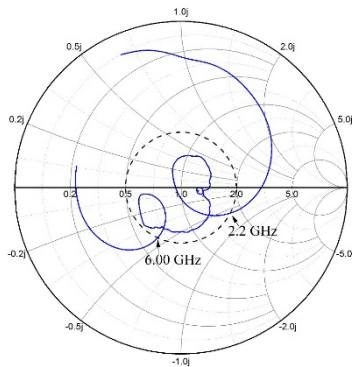


Fig. 18. Measured smith-chart of the proposed antenna

With respect to the physical dimension of the antenna by using the following equation [19, 20], the minimum quality factor can be achieved $Q_{lb} = \eta Q$ where, $k = \frac{2\pi}{\lambda}$ and a denotes sphere radius which is minimum sphere enclosed to the antenna. The higher bound of the radiation efficiency is $(B\eta r)_{ub} = \frac{1}{\sqrt{2}} \left[\frac{1}{ka} + \frac{1}{k^3 a^3} \right]^{-1}$. The Q_m and $(B\eta r)_{ub}$ for different values of ka is shown in Fig. 19. We get the value of $ka=1.35$ for the 2nd resonant frequency. From the ideal curve, it is noticed that the minimum limit of Q_m is 0.83 and $(B\eta r)_{ub} = 0.57$. The quality factor of the prototype is estimated through,

$$Q_a = \frac{2\sqrt{\beta}}{B} \text{ Where, } \sqrt{\beta} = \frac{s-1}{2\sqrt{s}} \leq 1 \quad (4)$$

$s=2$ considered as the maximum accepted VSWR. The achieved Q_a of the proposed antenna is 0.70 and $(B\eta r)_{ub} = 0.62$ which indicate that the theoretical and achieved value is very close. This verifies that the antenna design is optimum.

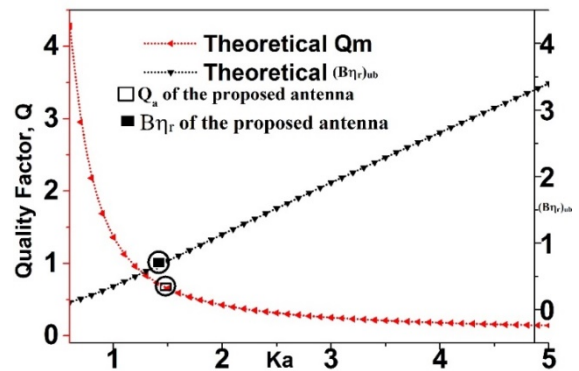


Fig. 19. Theoretical limits and calculated Q_a and $(B\eta r)_{ub}$

Table 3 compares the proposed and some existing antennas. The table shows that the proposed antenna achieves wider bandwidth and higher gain with a smaller size compared with the reported antennas, although some of the reported antennas obtain a wide bandwidth and higher gain compromising the overall size and structure.

Table 3. Comparison between proposed and some existing antennas

Author	Dimension (mm)	Bandwidth (MHz)	Fractional Bandwidth (%)	Peak gain (dBi)
[7]	53.7 × 53.7	1091	57.42	4.5
[9]	37 × 37	3120 (2230-5350)	80	4.7
[21]	85 × 85	8600(2.8-11.2)	120	5.5
[17]	70 × 70	2200 (3400-5600)	49.40	5.7
[22]	28 × 29	2730 (3.56–6.29)	55.43	3.74
[23]	80 × 80	3510	118.4	4.6
Proposed	36 × 36	3800(2200-6000)	92.68	3.65

5. Conclusion

In this article, the parasitic centre slotted patch into the rotated wide square slot antenna is presented for wideband applications with low-cost substrate. The impedance bandwidth of the proposed wide-slot antenna can be significantly enhanced by introducing the parasitic centre slotted patch in the ground plane and also, reduced the dimension of the proposed antenna. With the optimized dimension of the proposed antenna achieves -10dB impedance bandwidth of 92.68%. The proposed structure reveals an average peak gain of 3.65 dBi, above 92.58% average radiation efficiency, stable far-field radiation characteristics and low cross polarization in the entire operating bandwidth. By properly choosing the suitable slot shape position and tuning their dimensions parameter with simulation software, the proposed design with wide operating bandwidth, relatively small size, peak gain, improved radiation pattern and optimum Q factor are obtained. Therefore, the proposed antenna is feasible for use as low profile, a low-cost wideband antenna for wideband applications.

Acknowledgments

This work was supported by the University Kebangsaan Malaysia, Grant No. MI-2017-001 and GUP-2018-049.

References

- [1] C. A. Balanis, *Antenna Theory: Analysis and Design*: Wiley-Interscience, 2012.
- [2] B. Ma, X.-M. Yang, T.-Q. Li, H.-Y. Chen, H. He, Y.-W. Chen, et al., *Int. J. Appl. Electromagnet Mech.* **50**, 201 (2016).
- [3] F. G. Gharakhili, M. Fardis, G. R. Dadashzadeh, A. K. A. Ahmadi, N. Hojjat, *Progress in Electromagnetics Research* **68**, 161 (2007).
- [4] R. Azim, M. Samsuzzaman, T. Alam, M. Islam, M. Faruque, M. Zaman, et al., *Space Science and Communication (IconSpace)*, 2015 International Conference 402 (2015).
- [5] P. Li, J. Liang, X. Chen, *IEEE Trans. Antennas Propag.* **54**, 1670 (2006).
- [6] Y. Liu, K. Lau, Q. Xue, C. Chan, *IEEE Antennas Wirel. Propag. Lett.* **3**, 273 (2004).
- [7] J.-Y. Sze, K.-L. Wong, *IEEE Trans. Antennas Propag.* **49**, 1020 (2001).
- [8] T. Dissanayake, K. P. Esselle, *IEEE Trans. Antennas Propag.* **56**, 1183 (2008).
- [9] Y. Sung, *IEEE Trans. Antennas Propag.* **60**, 1712 (2012).
- [10] M. Samsuzzaman, M. Islam, *Microwave Opt. Technol. Lett.* **57**, 445 (2015).
- [11] R. Azim, M. T. Islam, N. Misran, *IEEE Antennas Wirel. Propag. Lett.* **10**, 1190 (2011).
- [12] M. T. Islam, R. Azim, A. T. Mobashsher, *Progress in Electromagnetics Research* **129**, 161 (2012).
- [13] A. Parvathy, T. Mathew, *Optoelectron. Adv. Mat.* **11**, 681 (2017).
- [14] M. Samsuzzaman, M. T. Islam, J. S. Mandeep, *Optoelectron. Adv. Mat.* **7**, 760 (2013).
- [15] W.-L. Chen, G.-M. Wang, C.-X. Zhang, *IEEE Trans. Antennas Propag.* **57**, 2176 (2009).
- [16] D. Krishna, M. Gopikrishna, C. Aanandan, P. Mohanan, K. Vasudevan, *IET Microwaves, Antennas & Propagation* **3**, 782 (2009).
- [17] J.-Y. Jan, J.-W. Su, *IEEE Trans. Antennas Propag.* **53**, 2111 (2005).
- [18] M. N. Rahman, M. T. Islam, S. Md. Samsuzzaman, *Microwave Opt. Technol. Lett.* **60**, 1681 (2018).
- [19] G. A. Mavridis, D. E. Anagnostou, M. T. Chryssomallis, *IEEE Antennas and Propagation Magazine* **53**, 216 (2011).
- [20] M. Z. Mahmud, M. T. Islam, M. N. Rahman, T. Alam, M. Samsuzzaman, *Int. J. Microw. Wirel. Technol.* **1** (2017).
- [21] P. Nageswara Rao, N. Sarma, *Microwave Opt. Technol. Lett.* **50**, 2820 (2008).
- [22] H.-R. Lee, J.-M. Woo, *8th International Symposium on Antennas, Propagation and EM Theory* 294 (2008).
- [23] Y. Sung, *IEEE Trans. Antennas Propag.* **59**, 3918 (2011).

*Corresponding author: samsuzzaman@siswa.ukm.edu.my